Published in final edited form as:
JACC Cardiovasc Imaging. 2013 May 01; 6(5): 600–9. doi:10.1016/j.jcmg.2012.09.019.

Assessment of Coronary Artery Stenosis Severity and Location: Quantitative Analysis of Transmural Perfusion Gradients by High-Resolution MRI Versus FFR

Amedeo Chiribiri, MD, PhD[*], **Gilion L. T. F. Hautvast, MSC, PhD**[†], **Timothy Lockie, BSc, MBChB, PhD**[‡], **Andreas Schuster, MD, PhD**[*,§], **Boris Bigalke, MD, PhD**[*], **Luca Olivotti, MD, PhD**[*,‖], **Simon R. Redwood, MD**[‡], **Marcel Breeuwer, PhD**[¶,#], **Sven Plein, MD, PhD**[**], **Eike Nagel, MD, PhD**[*]

[*]Division of Imaging Sciences and Biomedical Engineering, King's College London British Heart Foundation Centre of Excellence, National Institute for Health Research Biomedical Research Centre, and Wellcome Trust and Engineering and Physical Sciences Research Council Medical Engineering Centre at Guy's and St Thomas' NHS Foundation Trust, London, United Kingdom [†]Philips Group Innovation–Healthcare Incubators, Eindhoven, the Netherlands [‡]Cardiovascular Division, King's College London British Heart Foundation Centre of Excellence, and the National Institute for Health Research Biomedical Research Centre at Guy's and St Thomas' NHS Foundation Trust, St Thomas' Hospital, London, United Kingdom [§]Department of Cardiology and Pulmonology, Georg-August-University and German Center for Cardiovascular Research (DZHK, Partner Site), Göttingen, Germany [‖]Department of Cardiology, Santa Corona Hospital, Pietra Ligure, Italy [¶]Philips Healthcare, Imaging Systems–MR, Best, the Netherlands [#]Biomedical Engineering, Biomedical Image Analysis, Eindhoven University of Technology, Eindhoven, the Netherlands [**]Division of Cardiovascular and Neuronal Remodeling, University of Leeds, Leeds, United Kingdom

Abstract

Objectives—This study sought to test the hypothesis that transmural perfusion gradients (TPG) on adenosine stress myocardial perfusion cardiac magnetic resonance (CMR) predict hemodynamically significant coronary artery disease (CAD) as defined by fractional flow reserve (FFR).

Background—Myocardial ischemia affects the subendocardial layers of the left ventricular myocardium earlier and more severely than the outer layers, and the identification of TPG should be sensitive and specific for the diagnosis of CAD. Previous studies have shown that high spatial resolution myocardial perfusion CMR allows quantitation of TPG between the subendocardium and the subepicardium.

Methods—Sixty-seven patients (53 men, age 61 ± 9 years) underwent coronary angiography and high-resolution (1.2 × 1.2-mm in-plane) adenosine stress perfusion CMR at 3.0-T. TPG was

Correspondence to: Amedeo Chiribiri.

Reprint requests and correspondence: Dr. Amedeo Chiri- biri, King's College London, Division of Imaging Sciences, 4th Floor Lambeth Wing, St Thomas' Hospital, London SE1 7EH, United Kingdom. amedeo.chiribiri@lcl.ac.ul.

Europe PMC Funders Author Manuscripts

calculated for 3 coronary territories. Visual analysis was performed to identify myocardial ischemia. FFR was measured in all vessels with ≥50% severity stenosis. FFR <0.8 was considered hemodynamically significant. In a training group of 30 patients, the optimal threshold of TPG to detect significant CAD was determined (Group 1). This threshold was then tested prospectively in the remaining 37 patients (Group 2).

Results—In Group 1, a 20% TPG provided the best diagnostic threshold on both per-segment and per-patient analysis. Applied to Group 2, this threshold yielded a sensitivity of 0.78, specificity of 0.94, and area under the curve of 0.86 for the detection of CAD in a per-segment analysis and of 0.89, 0.83, and 0.86 in a per-patient analysis, respectively. TPG had a similar diagnostic accuracy to visual assessment. Linear regression analysis showed a relationship between TPG and FFR values, with $r = 0.63$ ($p < 0.001$).

Conclusions—The quantitative analysis of transmural perfusion gradients on high-resolution myocardial perfusion CMR accurately predicts hemodynamically significant CAD as defined by FFR. A TPG diagnostic threshold of 20% is as accurate as visual assessment. (J Am Coll Cardiol Img 2013;6: 600-9) © 2013 by the American College of Cardiology Foundation

Keywords

adenosine; coronary disease; fractional flow reserve; magnetic resonance imaging; perfusion

Myocardial ischemia affects the subendocardial layers of the left ventricular (LV) myocardium earlier and more severely than the outer layers (1). The high spatial resolution of myocardial perfusion cardiac magnetic resonance (CMR) allows the visualization of subendocardial ischemia as a delayed wash-in of the contrast agent (2–4). Postprocessing of perfusion CMR data can be used to quantify the imbalances between subendocardial and subepicardial myocardial perfusion. A novel method for semiautomated quantitative analysis of transmural perfusion gradients (TPG) has previously demonstrated a clear distinction between ischemic and normally perfused myocardium, with good reproducibility and good correlation with invasive coronary angiography (5). However, the diagnostic accuracy of myocardial TPG analysis against an appropriate functional endpoint has not been established yet.

Pressure wire— derived fractional flow reserve (FFR) is considered the invasive reference standard for assessing the functional significance of coronary stenoses and a better comparator for ischemia assessment than anatomical coronary angiography. The objective of this study was to determine whether TPG analysis can detect hemodynamically significant coronary artery disease (CAD) as defined by FFR in a prospective cohort of patients.

Methods

This study enrolled patients with suspected or known CAD. A first cohort of retrospectively enrolled patients were examined with a standard CMR perfusion protocol and underwent invasive coronary angiography and FFR assessment within 2 months of CMR (Group 1). Group 1 was used to identify the optimal thresholds of TPG for the detection of hemodynamically significant CAD defined by FFR <0.8 (6) on both a per-vessel and a per-patient analysis. According to clinical practice in our institution, FFR was performed in all

vessels with ≥50% luminal stenosis. Total coronary occlusions were regarded as significant lesions. Lesions with <50% luminal stenosis or with >50% stenosis but FFR ≥0.8 were considered not significant.

The optimal threshold derived in Group 1 was subsequently applied to a prospective verification group (Group 2) of consecutive patients listed for coronary angiography by clinical indication. All patients in Group 2 underwent perfusion CMR as part of the current study prior to coronary angiography.

Exclusion criteria were contraindications for CMR or gadolinium-based contrast agents, history of previous myocardial infarction, coronary artery bypass grafting, acute coronary syndrome, impaired LV function (ejection fraction <40%), and obstructive pulmonary disease. All subjects gave written informed consent in accordance with ethical approval. This study complies with the Declaration of Helsinki.

CMR protocol

CMR was performed at 3.0-T (Achieva-TX, Philips Healthcare, Best, the Netherlands) using a cardiac phased-array receiver coil. Perfusion data were acquired in 3 LV short-axis slices with a saturation-recovery gradient-echo method (repetition time/echo time 3.0 ms/1.0 ms, flip-angle 15°, saturation-recovery delay 120 ms, 5-fold *k-t* sensitivity encoding [*k-t* SENSE] acceleration with 11 training profiles, spatial resolution 1.2 × 1.2 × 10 mm^3) during adenosine-induced hyperemia (140 μg/kg/min) and 15 min later at rest using 0.05 mmol/kg of bodyweight gadolinium extracellular contrast agent (Magnevist, Bayer Schering Pharma, Berlin, Germany) injected at 4 ml/s followed by a 20-ml saline flush. Late gadolinium enhancement images were acquired 15 min after contrast was topped-up to a total dose of 0.2 mmol of gadolinium/kg of bodyweight (6).

Visual assessment of CMR perfusion

Studies were analyzed by 2 independent experts blinded to all other data (ViewForum, Philips Healthcare). A perfusion abnormality was defined as a delayed wash-in of the contrast agent in 1 or more segments compared with remote myocardium according to published methods (3). In case of disagreement between observers, the images were reviewed together and a consensus was reached.

TPG analysis

TPG analysis has been previously reported in detail (5). The implementation of highresolution signal intensity (SI) analysis in this study required accurate respiratory motion correction and myocardial contour delineation. Respiratory motion was corrected using affine image registration by maximization of the joint correlation between consecutive dynamics within an automatically determined region of interest. A temporal maximum intensity projection was then calculated to serve as a feature image for an automatic contour delineation method (5). The automatically generated contours were then optimized visually by the operator to carefully avoid areas of partial volume effect at the endocardial and epicardial border. The time required to optimize the segmentation and complete the TPG analysis time was recorded in the first 20 cases.

Following motion correction and contour delineation and optimization, myocardial SI curves were sampled using bilinear interpolation at a grid of 60 angular positions (Fig. 1).

The subendocardial and subepicardial SI curves, $\boldsymbol{I_{endo}}(\alpha,t)$ and $I_{epi}(\alpha,t)$ were obtained from the inner and outer thirds of the LV myocardium, ignoring the mid-wall layers to improve sensitivity to transmural differences in contrast uptake. The TPG curves $G(\alpha,t)$ were calculated based on the difference in myocardial SI values in the subendocardial and subepicardial layers for each dynamic t, normalized to the average transmural SI $I_{\text{transm}}(\alpha,t)$ in the same myocardial location α, and were expressed in percentage of transmural myocardial blood flow (MBF) redistribution (Equation 1).

$$G(a,t) = \frac{I_{epi}(\alpha,t) - I_{endo}(\alpha,t)}{I_{\text{trans}\ m}(\alpha,t)} \cdot 100\%$$

The normalized TPG curves represent the evolution of transmural gradients in contrast uptake over time.

To avoid analysis errors due to respiratory artifacts, the TPG analysis was restricted to the dynamic images starting with the upslope of the SI in the LV (T-onset) to the 15 following heartbeats (T-onset+ 15s).

Ischemic areas are detected based on the intensity of the TPG, which represents the difference in transmural perfusion between the endocardial and the epicardial layers (Fig. 2). TPG threshold values of 10%, 15%, 20%, and 25% were tested in Group 1. Each detected TPG was assigned to a coronary perfusion territory on the basis of the standardized LV segmentation (7) and compared with FFR. The best threshold identified on the receiver-operating characteristic (ROC) analysis in Group 1 was applied to Group 2 to verify its diagnostic accuracy in an independent population of patients. Intraobserver and interobserver variability of TPG analysis was assessed in Group 2 by comparing the results obtained by 2 operators blinded to the clinical and invasive data.

Catheter laboratory protocol

Invasive coronary angiography was performed with standard methods (8). FFR was measured in all vessels that showed a ≥50% diameter stenosis in 2 orthogonal views during intracoronary adenosine-induced hyperemia (140 μg/kg/min) with a 0.014-inch coronary pressure sensor-tipped wire (Volcano Therapeutics, San Diego, California or St. Jude Medical, St. Paul, Minnesota) (9).

Statistical analysis

Data were analyzed in a per-patient and per-vessel analysis. Data are presented as mean ± SD. Group means were compared using an unpaired Student t test. Categorical data were compared between groups using the Fischer exact test and Pearson chisquare test, as appropriate. ROC analysis was used to assess the diagnostic accuracy of TPG analysis and to determine the best TPG threshold. This was defined as the threshold with the highest sum of sensitivity and specificity. ROC analysis has been performed using log-transformed data. ROC curves were compared using the DeLong test (Medcalc, Medcalc Software, Ostend,

Belgium). Linear regression was used for correlation of TPG with FFR. Cohen's kappa was used to assess the intraobserver and interobserver reliability of qualitative (categorical) TPG results. Because 3 coronary artery territories were examined per patient, the intraclass correlation coefficient was calculated to determine the design effect and the need to adjust these data for clustering. The statistical analyses were performed using PASW software for Macintosh (IBM, Chicago, Illinois).

Results

CMR imaging

Thirty patients were enrolled in Group 1 and 37 patients in Group 2. The groups showed no difference in baseline demographics (Table 1).

Coronary angiography and FFR

Angiography was performed within 33 ± 26 days from the CMR study in Group 1 and 2.6 ± 5.1 days after CMR in Group 2, reflecting the different enrollment strategies ($p < 0.001$). Of the 90 vessels analyzed in Group 1, 35 (39%) showed a stenosis of more than 50% and were thus evaluated with FFR. Two vessels were chronically occluded in Group 1. Thirteen lesions had an FFR <0.8 (0.58 ± 0.17) and 22 lesions had an FFR ≥0.8 (0.89 ± 0.05; $p < 0.001$). In Group 2, 2 vessels were occluded and 42 of 111 vessels showed a visual stenosis >50% and were evaluated with FFR. Of these, 21 (50%) had FFR <0.80 (0.58 ± 0.16) and 21 (50%) had FFR ≥0.80 (0.90 ± 0.05; $p < 0.001$). No differences were found in the distribution and severity of the coronary lesions between the 2 groups (Table 2).

Visual assessment

When applied to Group 1, visual analysis yielded a sensitivity of 0.81 (95% confidence interval: 0.54 to 0.95), a specificity of 0.91 (0.81 to 0.96), positive predictive value (PPV) of 0.65 (0.41 to 0.84), and negative predictive value (NPV) of 0.96 (0.87 to 0.99) to detect coronary ischemia at a FFR <0.8, with an area under the ROC curve (AUC) of 0.9 (0.68 to 0.96) for vessel-based analysis. For patient-based analysis, visual assessment yielded a sensitivity of 0.92 (0.6 to 0.99), a specificity of 0.83 (0.58 to 0.96), a PPV of 0.79 (0.5 to 0.94), and a NPV of 0.94 (0.68 to 0.99) with an AUC of 0.86 (0.61 to 0.96). Similar results were found in Group 2, with a sensitivity of 0.78 (0.6 to 0.92), a specificity of 0.91 (0.82 to 0.96), a PPV of 0.69 (0.5 to 0.84), and a NPV of 0.94 (0.86 to 0.97) with an AUC of 0.85 (0.78 to 0.94) for vessel-based analysis, and a sensitivity of 0.89 (0.65 to 0.91), a specificity of 0.83 (0.58 to 0.96), a PPV of 0.85 (0.61 to 0.96), and a NPV of 0.88 (0.62 to 0.97) with an AUC of 0.86 (0.8 to 0.93) for patient-based analysis.

TPG analysis versus FFR

The analysis time for TPG quantitation was 5.4 ± 3.1 min per case. The main user interaction during TPG analysis was required to correct for imperfections in the automated image registration and segmentation, and to avoid partial volume effects at the endocardial and epicardial border.

For vessel-based analysis in Group 1, a threshold of 20% provided the optimal sensitivity (0.81; 0.54 to 0.95) and specificity (0.95; 0.86 to 0.98) to detect significant coronary lesions (AUC: 0.88; 0.76 to 1).

The 20% threshold yielded the best sensitivity (0.75; 0.43 to 0.93) and specificity (0.78; 0.52 to 0.92) to detect significant coronary lesions in Group 1 (AUC: 0.76; 0.58 to 0.95) also for patient-based analysis. Lower and higher threshold values gave less accurate results.

When applied to Group 2, the 20% threshold yielded the following results: sensitivity 0.78 (0.56 to 0.92), specificity 0.94 (0.87 to 0.98), PPV 0.78 (0.56 to 0.92), NPV 0.91 (0.82 to 0.96), and AUC 0.86 (0.76 to 0.97) for a per-vessel analysis, and sensitivity 0.89 (0.65 to 0.91), specificity 0.83 (0.58 to 0.96), PPV 0.85 (0.61 to 0.96), NPV 0.88 (0.62 to 0.98), and AUC 0.86 (0.73 to 0.99) (Fig. 3) for a per-patient analysis. TPG analysis had similar diagnostic accuracy to visual assessment on both a per-vessel and a per-patient analysis ($p = 0.89$ and $p = 1$, respectively).

Segments supplied by vessels with FFR <0.8 had higher TPG values (30 ± 14%) compared with segments supplied by vessels with FFR ≥0.8 (7.9 ± 6.9%; $p < 0.0001$) and vessels with no lesions or angiographic lesions <50% (5.5 ± 6.8%; $p < 0.0001$). No differences in TPG values were observed when comparing these last 2 groups ($p = 0.17$).

In vessels with high-grade coronary stenosis (FFR values of 0.3 to 0.35; n = 6), the average TPG was 36 ± 9% (range 24% to 42%). In vessels with chronic total occlusion (n = 5), the measured TPG was 57 ± 25% (range 22% to 84%) (Fig. 4).

Linear regression analysis showed a relationship between TPG and FFR values, with $r = 0.63$ (0.47 to 0.75; $p < 0.0001$) (Fig. 5).

Vessels supplying gradient-positive perfusion territories had FFR values significantly lower than gradient-negative perfusion territories (0.59 ± 0.2 vs. 0.86 ± 0.12, respectively; $p < 0.001$).

When comparing TPG analysis and visual assessment, the results were discordant in 4 patients in Group 2, with 2 false positives for each method: 1 patient with single-vessel disease (right coronary artery [RCA], FFR 0.94) and 1 patient with 2-vessel disease (left anterior descending coronary artery [LAD] and RCA, FFR 0.91 and 0.84, respectively) for TPG analysis and 1 patient with single-vessel disease (LAD, FFR 0.9) and 1 patient with 2-vessel disease (LAD and RCA, FFR 0.87 and 1, respectively) for visual assessment.

TPG analysis showed a good intraobserver and interobserver agreement for both vessel-based ($\boldsymbol{k} = 0.84$; 0.76 to 1, and $\boldsymbol{k} = 0.72$; 0.50 to 0.95, respectively) and patient-based analyses ($\boldsymbol{k} = 0.79$; 0.72 to 0.96, and $\boldsymbol{k} = 0.69$; 0.49 to 0.91, respectively). The intra-assay of the coefficient of variation of gradients positivity was 4% ($p = 0.32$) when cluster size was 3.

Four patients (2 in each group) had evidence of subendocardial myocardial infarction on late gadolinium-enhanced images. In 1 case, the presence of subendocardial scar caused a false-

positive TPG detected by the algorithm at thresholds of 10% and 15%. No false-positive TPG were identified at the threshold of 20%.

Discussion

The main findings of this study are: 1) quantitative TPG analysis of stress myocardial perfusion CMR data can be used to detect and localize hemodynamically significant CAD as defined by FFR; 2) a 20% TPG provides the optimal threshold for the detection of significant CAD for both vessel- and patient-based analyses; and 3) a 20% TPG has a similar diagnostic accuracy as visual assessment of perfusion CMR images.

Previous studies

The detection of subendocardial ischemia is considered a sensitive endpoint for the diagnosis of pathological alterations of myocardial blood supply (2,4,10–13). Previous studies have used single-photon emission computed tomography (SPECT) and positron emission tomography to measure the transmural perfusion ratio. Due to the relatively low spatial resolution of nuclear myocardial perfusion imaging, these studies have been limited to patients with LV hypertrophy (4,14–17). Only a few studies using ^{15}O-labeled water positron emission tomography reported a transmural perfusion ratio in normal hearts in animal experiments and in healthy volunteers (4), confirming the existence of transmural perfusion inhomogeneities also in normal hearts, with higher rest MBF in the subendocardium and a homogeneous MBF during stress.

Two studies have used the higher spatial resolution of multislice computed tomography (MSCT) to delineate transmural perfusion gradients. George et al. (18) described transmural differences in the attenuation density in the subendocardial and subepicardial layers of the LV during adenosine stress MSCT. Signals were sampled from a single perfusion image in the inner and outer thirds of the LV wall. The transmural perfusion ratio was inversely correlated with the percent diameter stenosis, providing functional information complementary to the anatomic diagnostic information by MSCT coronary angiography (18). Hosokawa et al. (19) compared MSCT-detected transmural perfusion abnormalities with SPECT and invasive coronary angiography. MSCT-derived transmural perfusion gradients were defined as the difference in attenuation density between the subendocardial and subepicardial layers, normalized to the LV wall thickness (Hounsfield unit/mm). The transmural perfusion gradients correlated with the severity of myocardial perfusion abnormalities detected by SPECT and yielded a higher diagnostic accuracy than SPECT compared with invasive coronary angiography.

The main advantages of CMR are its high spatial resolution and tissue contrast, and the lack of ionizing radiation (20). Previous studies have reported the use of the transmural perfusion ratio to explore the physiological transmural gradient of myocardial perfusion in healthy subjects (10,21) and to investigate the presence of ischemia in patients with syndrome X (2,12,22), cardiac transplant arteriopathy (11), and systemic inflammatory diseases (23,24). In these studies, CMR findings have been compared with coronary angiography anatomical findings (11,22,23), visual (22,24) or semiquantitative CMR perfusion indexes (2,12,23), and only in a few studies against MBF quantification (10,21) or invasive coronary flow

Europe PMC Funders Author Manuscripts

reserve measurements (11). All these studies but 1 (12) confirmed the relevance of subendocardial ischemia for the functional assessment of inducible perfusion abnormalities.

Present study

Our study confirms the diagnostic potential of TPG analysis and adds to the literature in several aspects. This is the first study to our knowledge validating subendocardial ischemia detection against FFR. All previous studies used stenosis severity on angiography as an endpoint, although it is well documented that the functional relevance of a given stenosis varies widely (25).

Recently, quantitative MBF analysis has become a widely adopted investigational method in the literature and high-resolution quantitative analysis is a competing technique with TPG analysis for the identification of subendocardial ischemia (26,27). However, the accuracy of MBF quantification can be affected by sampling errors in the arterial input function, by dispersion of the bolus of contrast exacerbated by an epicardial stenosis and by systematic errors in the fitting procedure required to calculate the MBF estimates (28). The TPG analysis has several practical advantages over MBF quantification. Unlike most other semiquantitative or quantitative analysis methods, it does not require administration of a diluted pre-bolus or the acquisition of rest perfusion images and is potentially more robust. Because TPG are normalized to the average transmural myocardial SI, the measurements are relatively insensitive to image inhomogeneities due to variations in the B1 field and different coil configurations, different schemes of contrast agent administration, field strength, and the acquisition pulse sequence (5). In the current study, this was reflected in the high interobserver reproducibility. Other analysis techniques, such as MBF quantification, are on the other hand more susceptible to field inhomogeneities (10).

Finally, unlike MSCT and nuclear techniques, the gradientogram method integrates the information acquired over the entire first myocardial contrast passage. This allows the visualization of the temporal evolution of the TPG from the upslope of signal in the LV cavity (T-onset) to the following 15 dynamics (T-onset+15s). This property, as well as the use of a threshold of intensity of the TPG as main diagnostic criterion, allows an effective filtering of the noise contained in the images that could be responsible for false positives, resulting in a good specificity on pervessel analysis at the cost of some false negatives. However, on a per-patient analysis, this property allowed a good diagnostic accuracy with balanced sensitivity and specificity.

A transmural redistribution of myocardial perfusion of 20% resulted in being the most accurate TPG threshold to detect hemodynamically significant CAD with very good diagnostic accuracy in both groups.

Study limitations

A theoretical limitation of TPG methods is that they may be false normal in the presence of high-grade coronary stenosis with consequent transmural ischemia. Interestingly, this situation did not arise in our patients, despite the presence of subjects with high-grade coronary stenoses and FFR values as low as 0.3, and patients with chronic coronary occlusions, for whom a visually transmural perfusion abnormality was reported. This

suggests that even high-grade stenoses do not cause truly transmural perfusion defects and that this can be demonstrated with TPG analysis if the source data have sufficient spatial and temporal resolution. Future studies will be required to demonstrate the feasibility of transmural perfusion gradient analysis also at 1.5-T with a lower in-plane spatial resolution. Future studies also need to evaluate the impact of collateral flow on TPG.

We have used a FFR cutoff of 0.8 (29), but 0.75 is also clinically used to define the significance of a coronary stenosis. We repeated the analysis for a cutoff of 0.75 (data not shown) without significant differences in the findings.

Our patient population had high disease prevalence, and future studies need to test the TPG method in other patient groups. We also excluded patients with a history of myocardial infarction because measurements of FFR in the infarct-related artery may potentially be biased for 2 reasons: 1) the mass of viable myocardium depending on the stenotic infarct-related artery is smaller for a similar degree of stenosis and 2) microvascular resistance may be greater in the infarcted area than in the reference area, possibly blunting maximal hyperemia (30). This choice has resulted in a very low prevalence of myocardial scar on late gadolinium enhancement images in the current study population. Areas of subendocardial scar are likely to generate false-positive TPG. This was observed in 1 case in Group 1, where an area of inferolateral subendocardial scar resulted in a positive gradient for thresholds between 10% and 15%. No falsepositive gradients were observed for the 20% threshold.

Our results also demonstrate a significant correlation between TPG and FFR values. However, several physiological factors such as the amount of collateral flow, microvascular reactivity, and myocardial contractile function are in principle capable to modulate the relationship between TPG and FFR and can explain the observed degree of correlation (r = 0.63).

Conclusions

The quantitative analysis of transmural perfusion gradients on high-resolution CMR accurately predicts hemodynamically significant CAD as defined by FFR.

Acknowledgments

The Centre of Excellence in Medical Engineering is funded by the Wellcome Trust and the Engineering and Physical Sciences Research Council (EPSRC) under grant number WT 088641/Z/09/Z. Dr. Lockie was funded by a British Heart Foundation Clinical Research Training Fellowship (FS/08/058/25305). Dr. Schuster received grant support from the British Heart Foundation (BHF) (grants RE/08/003 and FS/10/029/28253) and the Biomedical Research Centre (grant BRC-CTF 196). Dr. Plein was funded by a Wellcome Trust Research Fellowship during the early phase of this study (WT078288) and is currently funded by a British Heart Foundation Senior Research fellowship (FS/10/62/28409). The authors acknowledge financial support from the Department of Health via the National Institute for Health Research comprehensive Biomedical Research Centre award to Guy's & St Thomas' NHS Foundation Trust in partnership with King's College London and King's College Hospital NHS Foundation Trust. Dr. Chiribiri receives grant support from Philips Healthcare. Drs. Breeuwer and Hautvast are employees of Philips Healthcare. Dr. Plein receives grant support from Philips Healthcare. Dr. Nagel received significant grant support from Bayer Schering Pharma and Philips Healthcare. Drs. Plein and Nagel contributed equally to this work.

Abbreviations And Acronyms

AUC	area under the curve

CAD	coronary artery disease
CMR	cardiac magnetic resonance
FFR	fractional flow reserve
LAD	left anterior descending coronaryartery
LV	left ventricular
MBF	myocardial blood flow
MSCT	multislice computed tomography
NPV	negative predictive value
PPV	positive predictive value
RCA	right coronary artery
ROC	receiver-operating characteristic
SPECT	single-photon emission computed tomography
TPG	transmural perfusion gradient

References

1. Algranati D, Kassab GS, Lanir Y. Why is the subendocardium more vulnerable to ischemia? A new paradigm. Am J Physiol Heart Circ Physiol. 2011; 300 H1090-100 [PubMed: 21169398]
2. Panting JR, Gatehouse PD, Yang G-Z, et al. Abnormal subendocardial perfusion in cardiac syndrome X detected by cardiovascular magnetic resonance imaging. N Engl J Med. 2002; 346:1948–53. [PubMed: 12075055]
3. Lockie T, Ishida M, Perera D, et al. High-resolution magnetic resonance myocardial perfusion imaging at 3.0-Tesla to detect hemodynamically significant coronary stenoses as determined by fractional flow reserve. J Am Coll Cardiol. 2011; 57:70–5. [PubMed: 21185504]
4. Vermeltfoort IA, Raijmakers PG, Lubberink M, et al. Feasibility of subendocardial and subepicardial myocardial perfusion measurements in healthy normals with (15)O-labeled water and positron emission tomography. J Nucl Cardiol. 2011; 18:650–6. [PubMed: 21519976]
5. Hautvast GLTF, Chiribiri A, Lockie T, Breeuwer M, Nagel E, Plein S. Quantitative analysis of transmural gradients in myocardial perfusion magnetic resonance images. Magn Reson Med. 2011; 66:1477–87. [PubMed: 21630344]
6. Kramer C, Barkhausen J, Flamm S, Kim R, Nagel E. Standardized cardiovascular magnetic resonance imaging (CMR) protocols, Society for Cardiovascular Magnetic Resonance: Board of Trustees Task Force on Standardized Protocols. J Cardiovasc Magn Reson. 2008; 10:35. [PubMed: 18605997]
7. Cerqueira MD, Weissman NJ, Dilsizian V, et al. Standardized myocardial segmentation and nomenclature for tomographic imaging of the heart: a statement for healthcare professionals from the Cardiac Imaging Committee of the Council on Clinical Cardiology of the American Heart Association. Circulation. 2002; 105:539–42. [PubMed: 11815441]
8. Perera D, Biggart S, Postema P, et al. Right atrial pressure: can it be ignored when calculating fractional flow reserve and collateral flow index? J Am Coll Cardiol. 2004; 44:2089–91. [PubMed: 15542298]

9. Pijls NH, De Bruyne B, Peels K, et al. Measurement of fractional flow reserve to assess the functional severity of coronary-artery stenoses. N Engl J Med. 1996; 334:1703–8. [PubMed: 8637515]
10. Muehling O, Jerosch-Herold M, Panse P, et al. Regional heterogeneity of myocardial perfusion in healthy human myocardium: assessment with magnetic resonance perfusion imaging. J Cardiovasc Magn Reson. 2004; 6:499–507. [PubMed: 15137334]
11. Muehling OM, Wilke NM, Panse P, et al. Reduced myocardial perfusion reserve and transmural perfusion gradient in heart transplant arteriopathy assessed by magnetic resonance imaging. J Am Coll Cardiol. 2003; 42:1054–60. [PubMed: 13678930]
12. Vermeltfoort IAC, Bondarenko O, Raijmakers PGHM, et al. Is subendocardial ischaemia present in patients with chest pain and normal coronary angiograms? A cardiovascular MR study. Eur Heart J. 2007; 28:1554–8. [PubMed: 17504803]
13. Cheung SC, Chan CW. Cardiac magnetic resonance imaging: choice of the year. Circ J. 2011; 75:724–31. [PubMed: 21301137]
14. Miyai N, Kawasaki T, Taniguchi T, Kamitani T, Kawasaki S, Sugihara H. [Exercise-induced ST-segment depression and myocardial ischemia in patients with hypertrophic cardiomyopathy: myocardial scintigraphic study]. Japanese J Cardiol. 2005; 46:141–7. [PubMed: 16252566]
15. Kawasaki T, Akakabe Y, Yamano M, et al. Gated single-photon emission computed tomography detects subendocardial ischemia in hypertrophic cardiomyopathy. Circ J. 2007; 71:256–60. [PubMed: 17251677]
16. Ruijs WL, Hautvast JL, Akkermans RP, Hulscher ME, van der Velden K. The role of schools in the spread of mumps among unvaccinated children: a retrospective cohort study. BMC Infect Dis. 2011; 11:227. [PubMed: 21864363]
17. Rajappan K, Rimoldi OE, Dutka DP, et al. Mechanisms of coronary micro-circulatory dysfunction in patients with aortic stenosis and angiographically normal coronary arteries. Circulation. 2002; 105:470–6. [PubMed: 11815430]
18. George RT, Arbab-Zadeh A, Miller JM, et al. Adenosine stress 64- and 256-row detector computed tomography angiography and perfusion imaging: a pilot study evaluating the transmural extent of perfusion abnormalities to predict atherosclerosis causing myocardial ischemia. Circ Cardiovasc Imaging. 2009; 2:174–82. [PubMed: 19808590]
19. Hosokawa K, Kurata A, Kido T, et al. Transmural perfusion gradient in adenosine triphosphate stress myocardial perfusion computed tomography. CircJ. 2011; 75:1905–12. [PubMed: 21697608]
20. Ishida M, Morton G, Schuster A, Nagel E, Chiribiri A. Quantitative assessment of myocardial perfusion MRI. Curr Cardiovasc Imaging Rep. 2010; 3:65–73.
21. Radjenovic A, Biglands JD, Larghat A, et al. Estimates of systolic and diastolic myocardial blood flow by dynamic contrast-enhanced MRI. Magn Reson Med. 2010; 64:1696–703. [PubMed: 20928890]
22. Pilz G, Klos M, Ali E, Hoefling B, Scheck R, Bernhardt P. Angiographic correlations of patients with small vessel disease diagnosed by adenosine-stress cardiac magnetic resonance imaging. J Cardiovasc Magn Reson. 2008; 10:8. [PubMed: 18275591]
23. Ishimori ML, Martin R, Berman DS, et al. Myocardial ischemia in the absence of obstructive coronary artery disease in systemic lupus erythematosus. J Am Coll Cardiol Img. 2011; 4:27–33.
24. Kobayashi Y, Giles JT, Hirano M, et al. Assessment of myocardial abnormalities in rheumatoid arthritis using a comprehensive cardiac magnetic resonance approach: a pilot study. Arthritis Res Ther. 2010; 12 R171 [PubMed: 20836862]
25. Uren NG, Melin JA, De Bruyne B, Wijns W, Baudhuin T, Camici PG. Relation between myocardial blood flow and the severity of coronaryartery stenosis. N Engl J Med. 1994; 330:1782–8. [PubMed: 8190154]
26. Hsu LY, Groves DW, Aletras AH, Kellman P, Arai AE. A quantitative pixel-wise measurement of myocardial blood flow by contrast-enhanced firstpass CMR perfusion imaging. J Am Coll Cardiol Img. 2012; 5:154–66.

27. Zarinabad N, Chiribiri A, Hautvast GLTF, et al. Voxel-wise quantification of myocardial perfusion by cardiac magnetic resonance. Feasibility and methods comparison. Magn Reson Med. 2012; 68:1994–2004. [PubMed: 22354744]

28. Jerosch-Herold M. Quantification of myocardial perfusion by cardiovascular magnetic resonance. J Cardiovasc Magn Reson. 2010; 12:57. [PubMed: 20932314]

29. Tonino PAL, De Bruyne B, Pijls NHJ, et al. Fractional flow reserve versus angiography for guiding percutaneous coronary intervention. N Engl J Med. 2009; 360:213–24. [PubMed: 19144937]

30. Caymaz O, Tezcan H, Fak AS, Toprak A, Tokay S, Oktay A. Measurement of myocardial fractional flow reserve during coronary angioplasty in infarct-related and non-infarct related coronary artery lesions. J Invasive Cardiol. 2000; 12:236–41. [PubMed: 10825764]

Europe PMC Funders Author Manuscripts

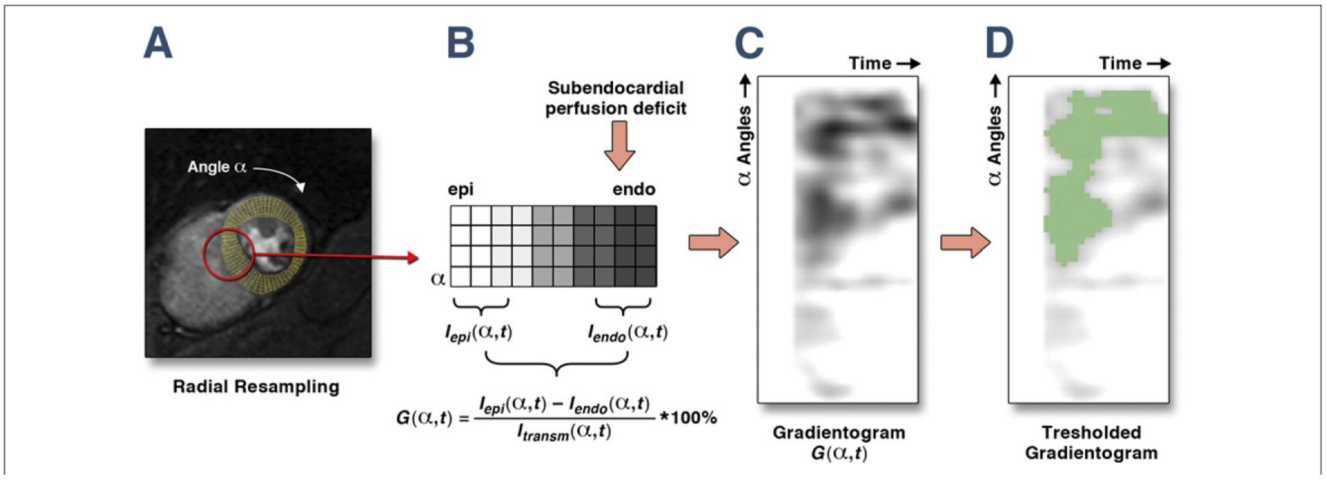

Figure 1. Schematic Representation of TPG Analysis

(A) After accurate motion correction and image registration, high-resolution perfusion series are segmented by drawing the endocardial (endo) and epicardial (epi) contour. By means of bilinear interpolation, data are resampled in 10 transmural layers and 60 radial segments per slice. **(B)** The algorithm calculates the intensity of the gradient G in each angular (α) and temporal position (t) by the spatial averaging of the SI of the inner (I_{endo}) and outer third (I_{epi}) of the LV wall, normalized by the average transmural SI (I_{trasm}) **(B)**. **(C)** The results are displayed on the gradientogram plot. The intensity of the gradient is represented by the **gray level** in each radial segment (y-axis) and for each temporal dynamic (x-axis). Increasing endocardial to epicardial gradients are represented with a **darkening gray level**, so that an endocardial perfusion defect generates a **dark area** in the gradientogram. **(D)** The gradientogram can be segmented at different percentage thresholds of the gradient's amplitude. In this case, an intensity threshold of 20% identifies a significant transmural perfusion gradient **(green area)**. LV = left ventricular; SI = signal intensity; TPG = transmural perfusion gradient.

Europe PMC Funders Author Manuscripts

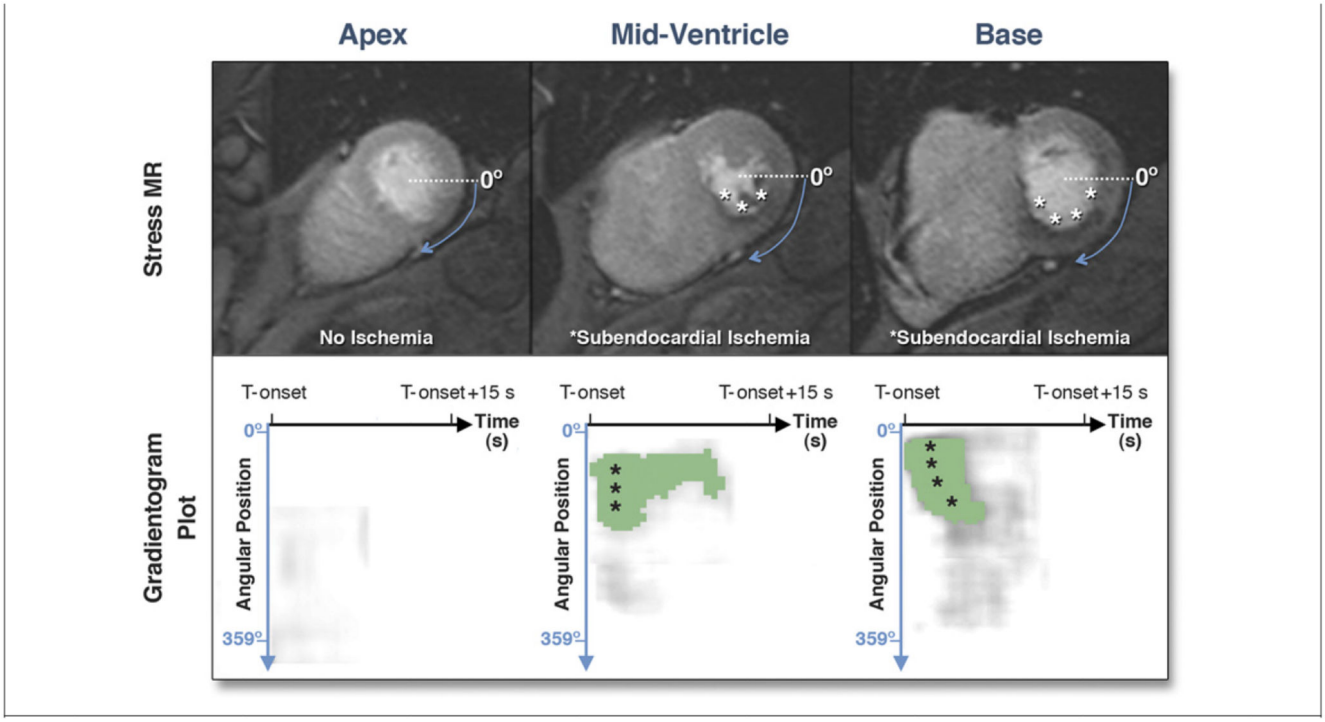

Figure 2. Example of TPG Analysis

Upper series, left to right: apical, mid-ventricular, and basal perfusion images at peak enhancement during first pass of gadolinium. The **asterisks** indicate a subendocardial perfusion defect in the inferior segments (no ischemia was seen on the apical slice in this case). Data are sampled in the radial direction starting from the 0° position, clockwise. **Lower series, left to right:** gradientogram plots segmented on a 15% threshold showing **green areas** of inducible TPG corresponding to areas of subendocardial ischemia in the corresponding CMR images. The angular position is represented on the y-axis. The time axis represents the evolution of the transmural perfusion gradient from the SI upslope in the left ventricle (T-onset) to the 15 following dynamic images (T-onset+15s). CMR = cardiac magnetic resonance; other abbreviations as in Figure 1.

Europe PMC Funders Author Manuscripts

Europe PMC Funders Author Manuscripts

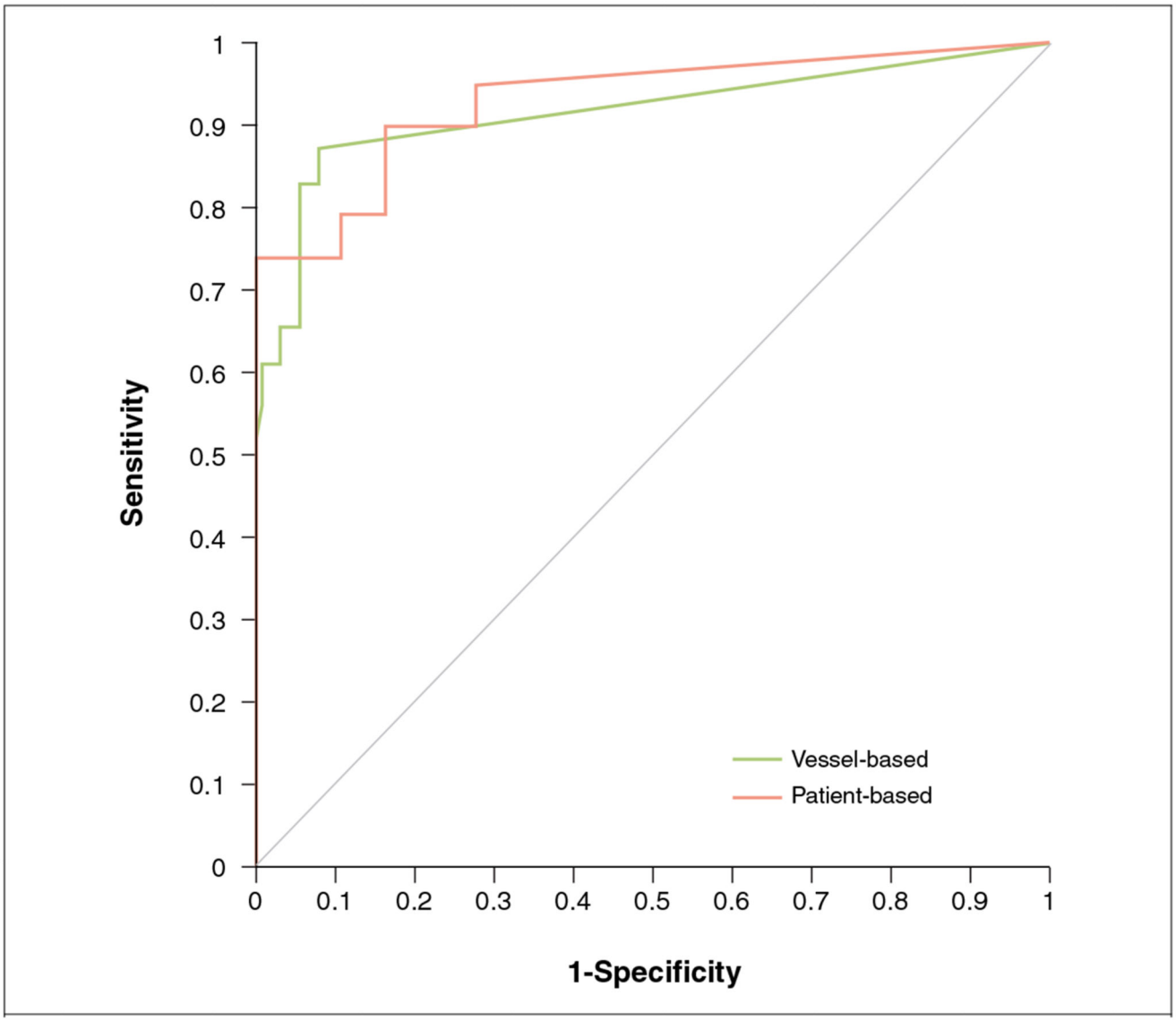

Figure 3. ROC Analysis for TPG Analysis on Per-Vessel and Per-Patient Analysis

When the best TPG threshold (20%) was applied to Group 2, it yielded a sensitivity of 0.78, specificity of 0.94, and area under the curve of 0.86 for a per-vessel analysis, and sensitivity 0.89, specificity 0.83, and area under the curve 0.86 for a per-patient analysis. ROC = receiver-operating characteristic; TPG = transmural perfusion gradient.

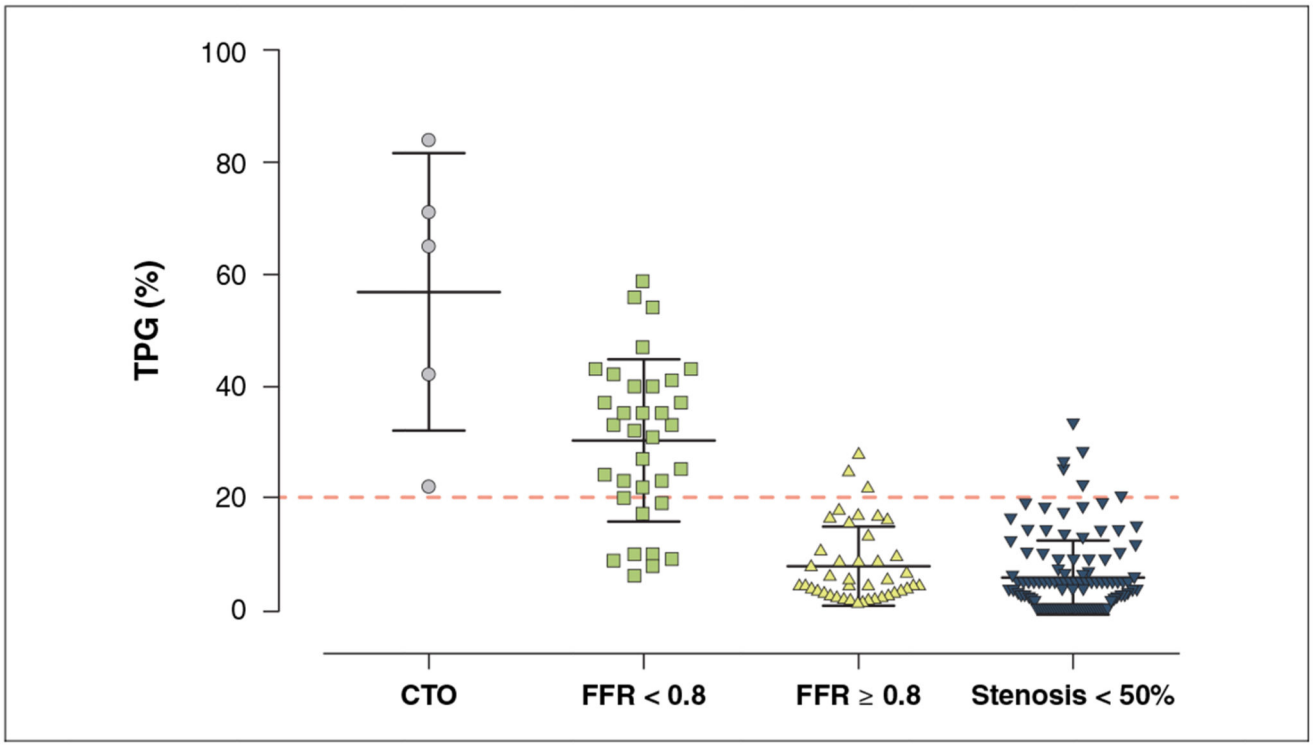

Figure 4. Scatterplot Showing the Distribution of TPG Values According to the Invasive Diagnosis

A progressive rise of TPG values was observed for increasing degrees of severity of coronary artery stenosis. Segments supplied by vessels with FFR <0.8 had higher TPG values compared with segments supplied by vessels with FFR ≥0.8 and vessels with no lesions or angiographic lesions <50%. The highest TPG values were measured in vessels with chronic total occlusion (CTO). FFR = fractional flow reserve; TPG = transmural perfusion gradient.

Europe PMC Funders Author Manuscripts

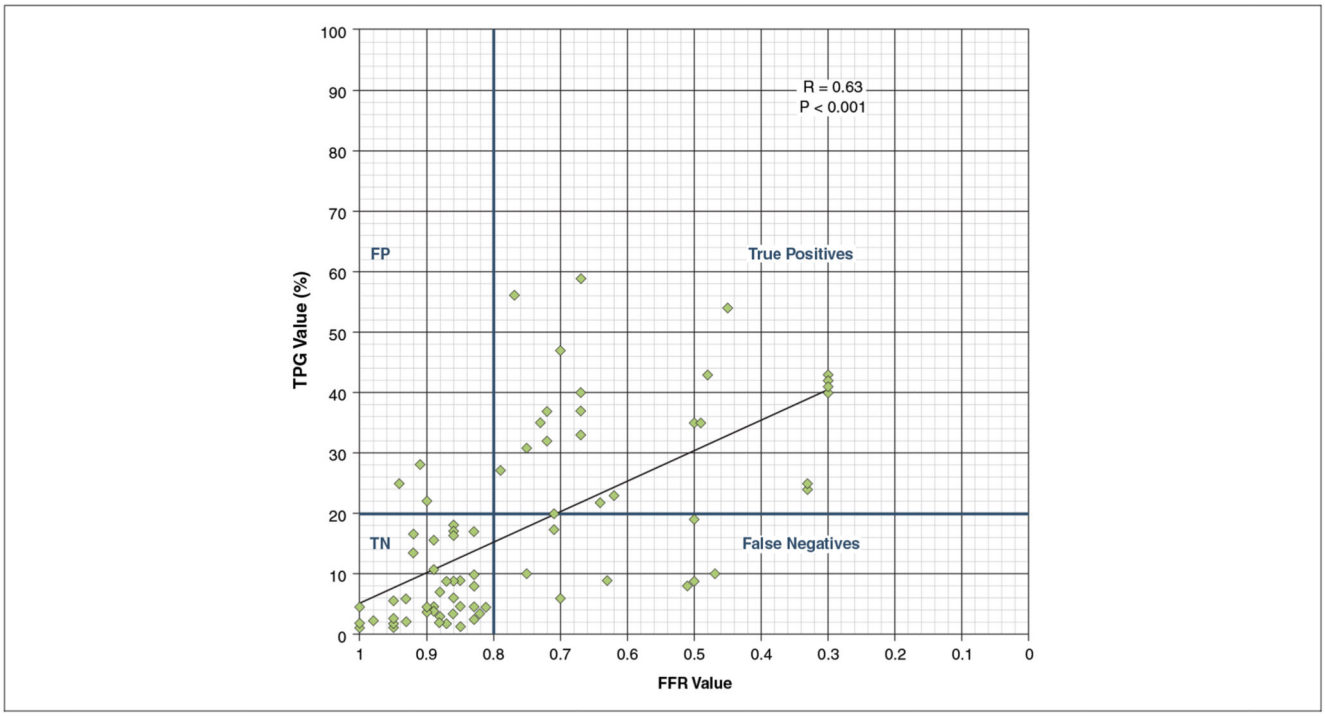

Figure 5. Scatterplot Showing the Distribution of TPG Values According to FFR

Linear regression analysis showed a relationship between TPG and FFR values. Several physiological factors such as the amount of collateral flow, microvascular reactivity, myocardial contractile function and the presence of subendocardial scar are in principle capable to modulate the relationship between TPG and FFR and can explain the observed degree of correlation, with r = 0.63 (0.47 to 0.75; p < 0.0001). Abbreviations as in Figure 4.

Europe PMC Funders Author Manuscripts

Europe PMC Funders Author Manuscripts

Table 1
Baseline Demographics of Patient Cohorts

	Group 1 (n = 30)	Group 2 (n = 37)	p Value
Male	22 (73)	31 (84)	0.48
Age, yrs	59 ± 11	62 ± 8	0.16
Previous PCI	6(20)	7 (19)	1.00
DM	8(27)	9 (24)	0.69
Previous stroke	2(7)	1 (3)	0.61
PVD	2 (7)	3 (9)	1.00
Smoker	8(27)	8 (22)	0.56
Family history of CAD	9 (30)	10 (27)	1.00
Medications			
Statin	23 (77)	30 (81)	0.67
Beta-blocker	13 (43)	19 (51)	0.43
Aspirin	27 (90)	32 (86)	0.72
Clopidogrel	14 (47)	17(46)	1.00
Nitrate	12(40)	16 (43)	1.00
Calcium channel blocker	6(20)	8 (22)	1.00
Nicorandil	1 (3)	2 (5)	1.00

Values are n (%) or mean ± SD.

CAD = coronary artery disease; DM = diabetes mellitus; PCI = percutaneous coronary interventions; PVD = peripheral vascular disease.

Europe PMC Funders Author Manuscripts

Table 2
Angiographic Findings in Both Patients' Cohorts

Per-Vessel Analysis	Group 1 (90 Vessels)	Group 2 (111 Vessels)	p Value
Vessels FFR measured	35/90 (39)	42/111 (38)	0.84
Vessels with FFR >0.80	22/35 (63)	21/42 (50)	0.37
Vessels with FFR <0.80	13/35 (37)	21/42 (50)	0.42
FFR negative vessels	0.89 ± 0.05	0.90 ± 0.05	0.44
FFR positive vessels	0.58 ± 0.17	0.58 ± 0.16	0.95
Vessels with FFR <0.80			
LAD	8/13 (62)	12/21 (57)	0.78
RCA	4/13 (31)	6/21 (29)	1.00
LCX	1/13 (8)	3/21 (14)	0.62
Vessels with chronic total occlusion	2/90 (2.2)	2/111 (1.8)	1.00
Per-Patient Analysis	**Group 1 (n = 30)**	**Group 2 (n = 37)**	**p Value**
Time from CMR scan, day	32 ± 25	2.5 ± 5	<0.001
Vessels FFR measured	1.17 ± 1.05	1.14 ± 0.8	0.85
No significant CAD	6/30 (20)	6/37 (16)	0.75
1-Vessel disease	11/30 (37)	18/37 (49)	0.39
2-Vessel disease	7/30 (23)	9/37 (24)	1.00
3-Vessel disease	4/30 (13)	2/37 (5)	0.22

Values are n/N (%) of each group or mean ± SD.

CAD = coronary artery disease; CMR = cardiac magnetic resonance: FFR = fractional flow reserve; LAD = left anterior descending coronary artery; LCX = left circumflex coronary artery; RCA = right coronary artery.